Journal of Materials Chemistry B

ROYAL SOCIETY OF CHEMISTRY

PAPER

View Article Online
View Journal | View Issue

Cite this: J. Mater. Chem. B, 2022, 10, 2471

A natural polysaccharide-based antibacterial functionalization strategy for liquid and air filtration membranes†

Ruonan Wu,‡ Mengkai Song,‡ Dandan Sui, Shun Duan* and Fu-Jian Xu *

Received 18th October 2021,
Accepted 11th November 2021

DOI: 10.1039/d1tb02273c

rsc.li/materials-b

Filtration membranes are widely applied in medical fields. However, these membranes are challenged by bacterial contamination in hospitals, which increases the risk of nosocomial infections. Thus, it is significant to develop antibacterial filtration membranes. In this work, an oxidated dextran (ODex)-based antibacterial coating was designed and constructed on microfiltration (MF) membranes and melt-blown fabrics. Polyhexamethylene guanidine (PHMG) was synthesized as an antibacterial agent, and was fixed by ODex onto filtration membranes. The functionalized MF membranes increased the filtration efficiency for *E. coli* from 20.9% to 99.9%, and improved the absorption ratio for endotoxin by 59.1%, while the water flow rate still remained as high as 5255 L (h m^2)$^{-1}$. Furthermore, the trapped bacteria were inactivated by the antibacterial coating. For the melt-blown fabrics, the aerosol filtration efficiency was increased from 74.6% to 81.0%, and the antibacterial efficiency was promoted to 92.0%. The present work developed a facile and universal antibacterial functionalization strategy for filtration membranes, which provided a new method for the design and development of various novel antibacterial filtration materials in the medical field.

1. Introduction

Pathogenic microorganisms extensively exist in air and water, which threaten the health of humans.[1–3] To defend the threats of such pathogens, filtration technology is an efficient method to eliminate the contaminants, such as solid particles and aerosols.[4,5] In particular, filtration membranes are widely used in the medical field, such as filtration sterilization, liquid transportation, sewage treatment, and air purification.[6–9] Furthermore, masks and other personal protective equipment (PPE) have played essential roles in fighting the epidemic of Coronavirus Disease-19 (COVID-19) for the past two years.[10] The filtration membranes are commonly manufactured by inert polymers, such as polyether sulfone (PES), polypropylene (PP), polyvinylidene difluoride (PVDF), and nylon.[11–14] These polymers could entrap the particles with retention effects by electrostatic absorption or the openings whose sizes are smaller than the particles. However, traditional polymer filtration membranes only work by physical retention effect. The retained pathogenic particles, such as bacteria, are still active on the surface of the filtration membrane, which may induce secondary contamination and cause harm to the health of the users.[15,16] Therefore, it is necessary to develop filtration membranes with high antibacterial efficiency.

Because the retained bacteria contact with the surface of the filtration membrane, antibacterial functionalization on the surface is a promising strategy to solve the problems of bacterial contamination. Compared with the bulk modification of the filter membrane, the surface functionalization strategy shows great advantages.[17] In the bulk modification of the material, it is often necessary to introduce other functional substances into the raw material, and it is necessary to take many issues into account, such as compatibility between matrices and additives, mechanical properties, and processability. On the contrary, surface functionalization only introduces a layer of functional substances on the surface of the filter membrane, thereby giving the surface new properties, which will hardly affect the mechanical properties of the material itself. The continuous development of surface modification technology provides unlimited possibilities for the development of multi-functional filter membranes, and enriches the application fields of filter materials.

By introducing antibacterial components onto the surface, the antibacterial properties could be improved. Poly(ethylene

Key Lab of Biomedical Materials of Natural Macromolecules (Beijing University of Chemical Technology), Ministry of Education, Beijing Laboratory of Biomedical Materials, Beijing Advanced Innovation Center for Soft Matter Science and Engineering, Beijing University of Chemical Technology, Beijing 100029, China. E-mail: duanshun@mail.buct.edu.cn, xufj@mail.buct.edu.cn

† Electronic supplementary information (ESI) available: Detailed experimental methods, the synthesis route of PHMG, the ^{1}H NMR spectrum of PHMG, the antibacterial efficiency of PHMG, element ratios of the pristine and modified PES MF membranes, element ratios of the pristine and modified PP melt-blown fabrics, and the bacterial filtration efficiency of PES–ODex–PHMG against *E. coli* with different density are provided in the Supporting Information. See DOI: 10.1039/d1tb02273c

‡ Both authors contributed equally to this work.

glycol) (PEG) and tannic acid–reduced gold nanoparticles (Au@TA NPs) were modified on the polydimethylsiloxane (PDMS) surface for better photothermal and antifouling performance.[18] Meanwhile, PDMS was deposited by TA–Ag NPs to achieve the antibacterial goal.[19] An *N*-halamine polymeric coating was modified on a titanium surface for long-lasting renewable antibacterial efficacy with good stability and biocompatibility.[20] P(DMAMS-*co*-PFDA) would be a promising anti-pathogenic polymeric coating on a polyester textile.[21] In addition, many antimicrobial modification strategies of the membranes have been reported. Polyethyleneimine was used to enhance the antimicrobial and filtering performances of PES filtration membranes by physical absorption.[22] By pad-dry technique, *N*-halamine-coated PP nonwoven fabrics were prepared, which showed high antibacterial property.[23] However, such noncovalent functionalization methods could not provide a stable antibacterial surface, and the detached antibacterial components would shorten the lifetime of the antibacterial activity and be harmful to the users, especially in PPE. To improve the stability of the antimicrobial activity, many covalent bonding-based techniques are well developed, such as surface-initiated polymerization and surface coupling.[24,25] Antibacterial MF membranes could be prepared by surface-initiated grafting polymerization and quaternization reaction of 4-vinylpyridine.[26] Silver nanoparticles were coupled onto the surface of the PES membranes by plasma treatment, which improved the antibacterial property and was applied for MF of milk.[27] By a layer-by-layer thiol–ene click reaction, the hydrogel coating could be constructed on the surface of the MF membrane for antimicrobial functionalization.[28] Nevertheless, facile and universal strategies for the antimicrobial filter membranes are still to be further developed. Polysaccharides, a kind of environment-friendly materials, have a wide range of sources and varieties, and the rich reactive functional groups provided plentiful sites for further chemical modification, which have been widely studied in biomedical materials.[29–33] Based on these previous works, antimicrobial functionalization of filtration materials with polysaccharide derivatives is a promising bioinspired surfaces engineering concept.

In this work, we developed a polysaccharide-based surface modification strategy for the antimicrobial functionalization of filter membranes (Scheme 1). PES membranes for water filtration and PP melt-blown fabrics for gas filtration were selected as representative filter membranes in the medical field. To introduce amino groups on the surface of the membranes, a silane coupling agent, 3-aminopropyl triethoxysilane (APTES), was applied. Then, oxidized dextran (ODex) was anchored through Schiff base bonds as the macromolecular backbone to prepare PES–ODex and PP–ODex. The antibacterial agent, polyhexamethylene guanidine (PHMG), was grafted onto the surface containing aldehyde groups through Schiff base bonds to obtain an antibacterial functionalized surface, PES–ODex–PHMG and PP–ODex–PHMG. Through the bacterial filtration experiment in the water environment, the PES filter membrane's ability to filter bacteria was evaluated. The surface antibacterial experiment was used to explore the membrane's ability to kill bacteria. In addition, the endotoxin adsorption experiment was used to evaluate the membrane's ability to adsorb endotoxin. We also evaluated the bacteria filtration efficiency (BFE) against aerosols through the filtration experiment, which explored the ability of melt-blown cloth to kill bacteria. The present work provided a facile and universal method for the antimicrobial functionalization of filter membranes.

2. Results and discussion

2.1 Physical and chemical characterizations

PHMG was synthesized with guanidine hydrochloride and hexamethylene diamine (Fig. S1, ESI†). The chemical structure of PHMG was confirmed by ^{1}H NMR spectrum with the solvent

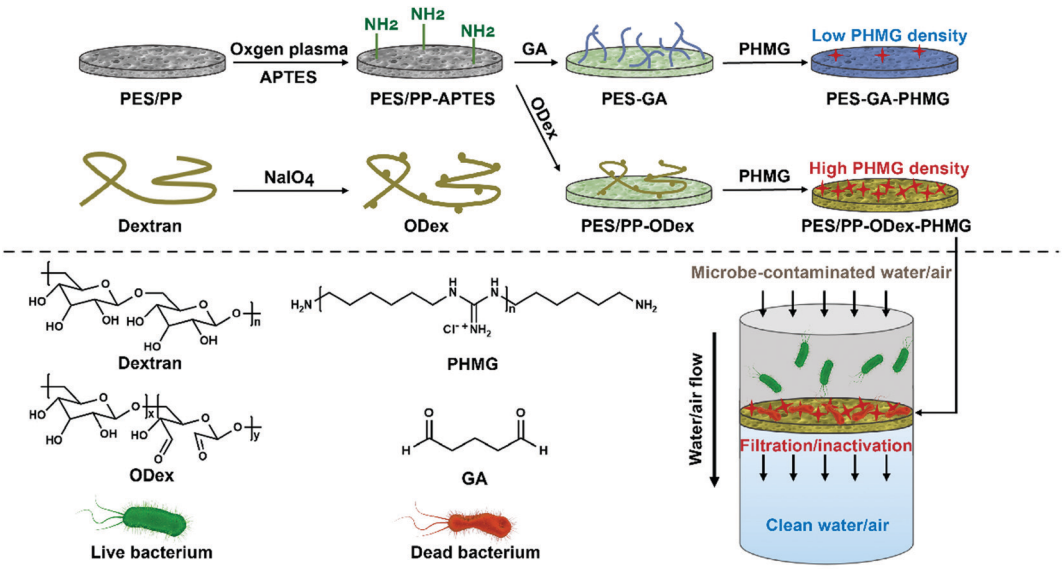

Scheme 1 The design strategy for the antimicrobial functionalization of filtration membranes.

of DMSO-d_6 (Fig. S2, ESI†). The peak at the chemical shift of 6.5–8.5 ppm was attributed to –N**H**– and –C=N**H**$_2^+$. The peak at 3.15 ppm was attributed to –C**H**$_2$–NH–. The peak at 1.46 ppm was attributed to –C**H**$_2$–CH$_2$–NH–. Finally, the peak at 1.31 ppm was attributed to –CH$_2$–C**H**$_2$–CH$_2$–. The ^{1}H NMR results proved the successful synthesis of the PHMG. The antibacterial efficiency of PHMB was tested by minimal bactericidal concentration (MBC) method (Fig. S3, ESI†). After co-culturing different concentrations of PHMG and bacteria with a bacterial density of 10^8 CFU mL^{-1} for 12 h, it was found that PHMG with the concentrations above 0.125 μg mL^{-1} could completely kill *E. coli* (ATCC 25922). The MBC against *S. aureus* (ATCC 25923) was 0.5 μg mL^{-1}. These results demonstrated that PHMG had excellent ability to kill Gram-negative bacteria and Gram-positive bacteria. At the same time, it was found that PHMG had a better ability to kill *E. coli* than *S. aureus*. PHMG killed bacteria by destroying the integrity of the bacterial cell membrane, and it also caused changes in the permeability of the bacterial surface and inhibited the activity of bacterial enzymes.[34] The effect of PHMG on the enzymes in *E. coli* was greater than that on *S. aureus*, which might be the reason why PHMG had better antibacterial properties against *E. coli*.[35] Due to its excellent antibacterial property and rich amino groups for Schiff base reactions, PHMG was selected as the antimicrobial component for surface functionalization of filter membranes.

The ratio of aldehyde groups in ODex was determined by hydroxylamine hydrochloride-potentiometric titration according to the hydroxylamine hydrochloride-potentiometric titration curve and the first-order differential curve (Fig. S4, ESI†). The aldehyde groups on ODex reacted with hydroxylamine hydrochloride to generate oxime and released HCl at the same time.[36] Based on Fig. S4 (ESI†), the degree of hydroformylation of ODex was calculated as 70%, which suggested that there were about 1.4 aldehyde groups on each glucose unit. At this feed ratio, the theoretical degree of hydroformylation was 90%. Therefore, the degree of reaction was calculated as 77%. Due to the high degree of hydroformylation, the abundant number of aldehyde groups provided rich reaction sites for the aminated surface, which was beneficial for the chemical grafting of ODex. At the same time, ODex acted as a macromolecular skeleton, and the rich aldehyde groups provided a large number of reaction sites for the amino groups of the antibacterial agent, PHMG.

The physical and chemical properties of functionalized PES membranes were first characterized. The morphologies of PES and PES–ODex–PHMG were observed by scanning electron microscope (SEM). Compared with the pristine PES membrane, the functional coating had not plug up the pores (Fig. 1a). This result showed that the grafted macromolecule, ODex, and small molecule antibacterial agents, PHMG, did not have a significant impact on the surface structure of the MF membrane. Furthermore, the functionalization process did not cause the pore blocking phenomenon of the MF membrane, which did not have negative effects on the filtration function of the MF membrane.

In order to prove the introduction of amino groups, aldehyde groups and PHMG, the surface zeta potential of each sample was tested (Fig. 1b). The zeta potential of PES was nearly neutral. After APTES treatment, the potential increased to 40 mV, showing a higher positive potential. This was due to the introduction of –NH$_2$ on the surface of the MF membrane. For comparison with

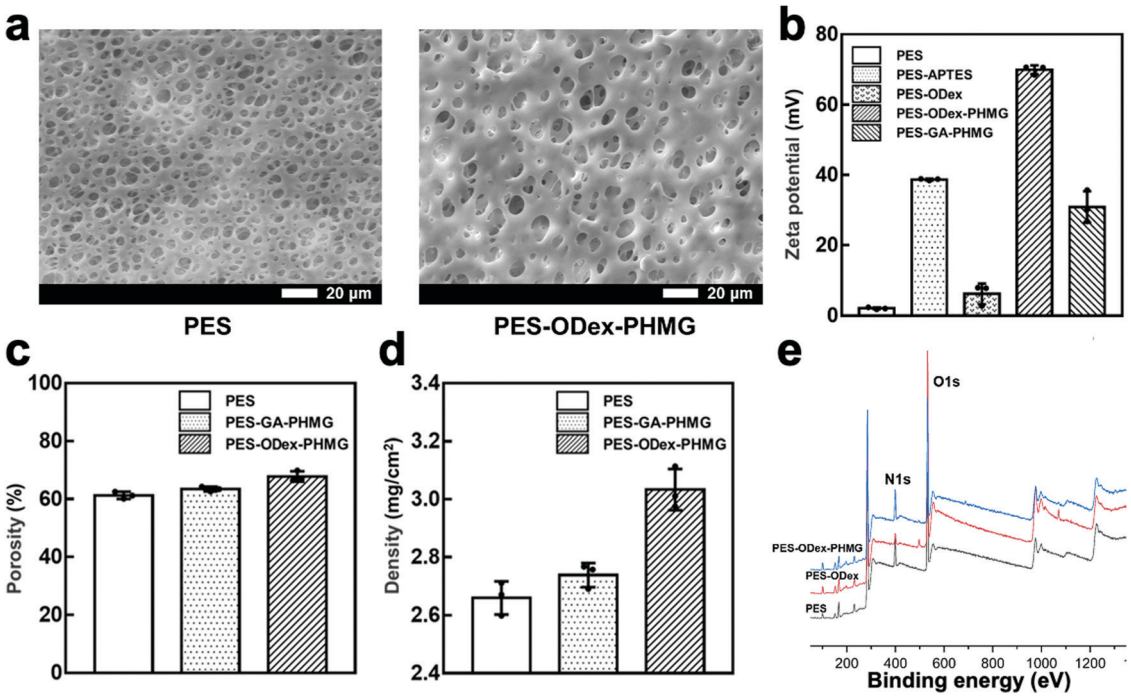

Fig. 1 (a) SEM images of PES and PES–ODex–PHMG; (b) surface zeta potentials of the pristine and functionalized MF membranes; porosity (c), density (d) and XPS wide-scan spectra (e) of the pristine PES and functionalized samples.

the macromolecular skeleton, ODex, a small molecule aldehyde, glutaraldehyde (GA), was taken as a control. The potential decreased to about 5 mV after grafting ODex, which was due to the introduction of aldehyde groups on the surface. In the ODex group, a large number of aldehyde groups reacted with $-NH_2$ through the Schiff base reaction, which reduced the positive charge. The zeta potential of PES–ODex–PHMG rose sharply to about 70 mV, because the strong positively charged guanidine groups were introduced to the surface. On the contrary, the zeta potential of PES–GA–PHMG was about 30 mV, which showed that GA, as a small molecule, was less efficient for the surface grafting of PHMG than the macromolecule, ODex.

The porosity of the MF membrane before and after the functionalization was determined by weighing method (Fig. 1c). Compared with the pristine PES membrane (61.3%), the porosity of PES–GA–PHMG (63.5%) and PES–ODex–PHMG (67.8%) were both slightly increased. The increase in porosity might be due to the hydrophilicity of PHMG. PES–ODex–PHMG exhibited a higher porosity than PES–GA–PHMG, because the ODex provided more reaction sites for PHMG than GA. In addition, when measuring the dry masses of the functionalized PES membranes, it was found that the masses were higher than that of the pristine PES membranes (Fig. 1d). This result was attributed to the grafted components. Compared with pristine PES, the mass of PES–GA–PHMG increased by 3%, while the mass of PES–ODex–PHMG increased by 14%. This result further illustrated that with the natural polysaccharide derivative, ODex, as the macromolecular skeleton, PHMG has a higher grafting density onto the surface of the MF membrane.

To further analyze the chemical property of the samples, X-ray photoelectron spectroscopy (XPS) was used to characterize the element contents of the surface of PES, PES–ODex and PES–ODex–PHMG (Fig. 1e). The XPS spectra are shown in Fig. 1e, and the ratio of each element is listed in Table S1 (ESI†). Compared with PES, the O element content on the surface of PES–ODex increased from 15.31% to 28.14%, which proved the successful introduction of ODex. Furthermore, the N element content on the surface of PES–ODex–PHMG increased from 2.98% to 8.03% compared with PES–ODex, which demonstrated the successful introduction of PHMG. The results of the physical and chemical characterization proved that the antibacterial component, PHMG, was grafted onto the surface of the PES MF membranes with a high density.

Through a similar strategy, surface functionalization of PP melt-blow fabrics was performed. The SEM images showed that the surface morphology of PP–ODex–PHMG did not change significantly, indicating that the fiber structure of the melt-blown fabrics was not significantly damaged (Fig. 2a). Because the advantages of ODex over GA had been demonstrated on the surface of the PES MF membranes, the GA was not studied in the PP melt-blown fabrics. The surface potential of PP–APTES increased from −2.1 mV to 26.7 mV after oxygen plasma and

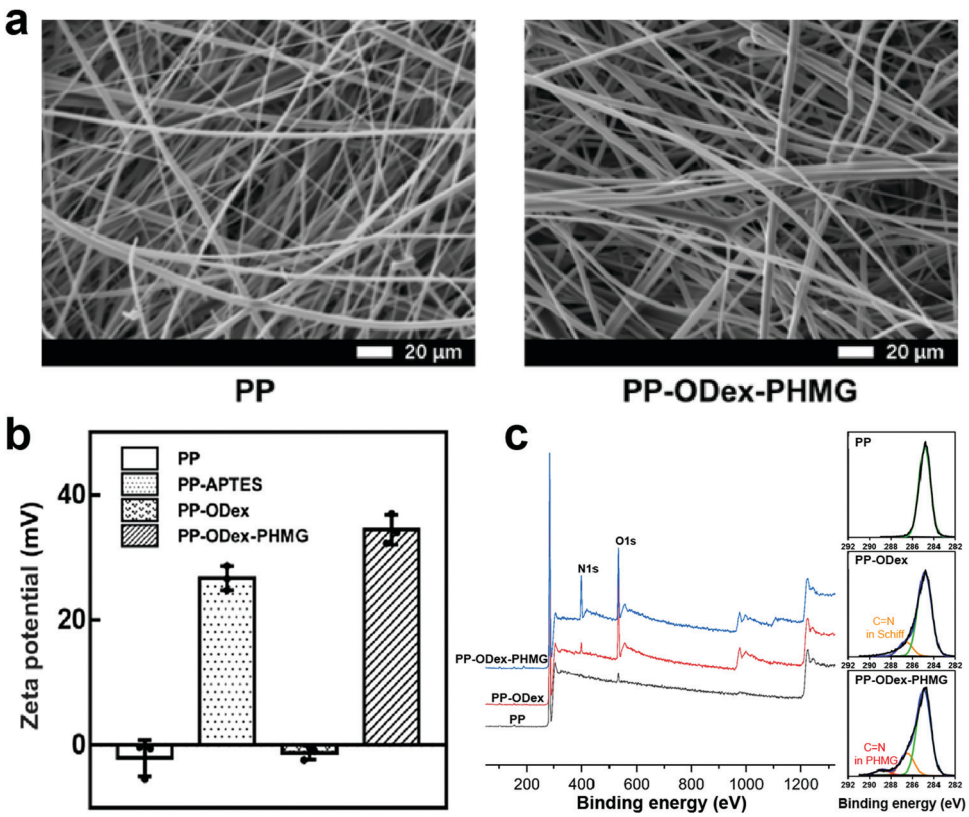

Fig. 2 (a) SEM images of the PP melt-blown fabric and PP–ODex–PHMG; (b) surface zeta potentials of the pristine and functionalized melt-blown fabrics; (c) XPS spectra of the pristine and functionalized melt-blown fabrics.

APTES treatment, which was due to the successful introduction of amino groups on the surface (Fig. 2b). Then, the surface potential of PP–ODex decreased to −1.2 mV, owing to the introduction of ODex. Finally, the surface potential of PP–ODex–PHMG increased to 34.4 mV, because PHMG was successfully grafted onto the aldehyde-based surface, and the guanidine groups provided a higher positive surface zeta potential. Compared with PP, the O 1s peak in the PP–ODex spectrum greatly increased, which corresponded to the increase in the content of O from 1.46% to 9.15% (Table S2, ESI†). This was due to the successful grafting of a large amount of ODex on the surface. After PHMG was grafted, the peak of N 1s at about 400 eV increased, and the N element content increased from 7.58% to 17.46%. A core-level spectrum of the carbon element showed that a new peak appeared at the binding energy of 286.7 eV in the PP–ODex group, which was attributed to the C═N bond in the Schiff base structure (Fig. 2c). Compared with PP–ODex, PP–ODex–PHMG had a new peak at 289.0 eV, which was the signal of the C═N bond in the guanidine group of PHMG, which proved that ODex and PHMG have been successfully introduced to the surface. These results demonstrated that PHMG could be introduced onto the surface of various types of filtration materials with a high density by the ODex-based strategy.

2.2 Filtration and antimicrobial properties of functionalized PES MF membranes

To test the water flow rate of PES MF membranes in the filtration process, a dead-end filter device was used to filter 1 kg of deionized water under gravity. Before and after the functionalization, the average water flux of the MF membrane was increased from 4093 L $(h\ m^2)^{-1}$ to 5255 L $(h\ m^2)^{-1}$ (Fig. 3a), which was attributed to the increase in porosity of the PES–ODex–PHMG MF membrane (Fig. 1c).

The pore size of the MF membrane directly affects the filtration efficiency, and the most direct method to increase the filtration rate is to increase the pore size of the MF membrane. However, when the pore size of the MF membrane exceeds the size of the bacteria, the MF membrane will lose its physical retention ability for microorganisms. Under this condition, when strong positively charged functional groups are introduced on the surface of the MF membrane, the negatively charged bacteria and other microorganisms will be adsorbed to the surface of the MF membrane by electrostatic interaction, which will obtain a high filtration rate without loss of the filtration performance.[37] To evaluate the filtration performance against bacteria, PES, PES–GA–PHMG and PES–ODex–PHMG were used to filter the *E. coli* suspension at the bacterial density of 4×10^5 CFU mL^{-1} under the driving force of gravity. The pristine PES could filter only 20.9% of the bacteria (Fig. 3b). Compared with PES, PES–GA–PHMG and PES–ODex–PHMG have significantly improved the filtration efficiency against *E. coli*, and the filtration efficiencies were increased to 65.2% and 99.9%, respectively. PES–ODex–PHMG showed higher filtration efficiency against bacteria than PES–GA–PHMG, which was attributed to the fact that ODex provided a large number of reaction sites. The macromolecular skeleton, ODex, enabled PHMG to be grafted to the surface of the MF membrane at a high density and promoted the filtration performance.

In order to further confirm the ability of the PES–ODex–PHMG to remove *E. coli* with different bacterial densities, the maximum filtration capacity of the PES–ODex–PHMG MF membrane was tested using a circular filtration method within 6 min (Fig. 3c). As the density of bacteria increased, the filtration efficiency of PES–ODex–PHMG against bacteria gradually decreased (Fig. 3d). Below 10^6 CFU mL^{-1}, PES–ODex–PHMG had an excellent filtering efficiency that was higher than 99.1%. Moreover, the amounts of intercepted bacteria were augmented with the increasing bacterial density, which showed that the ability of PES–ODex–PHMG to intercept bacteria was not affected by the high bacterial density (Table S3, ESI†). The decreased filtration ratios might be that when high-density

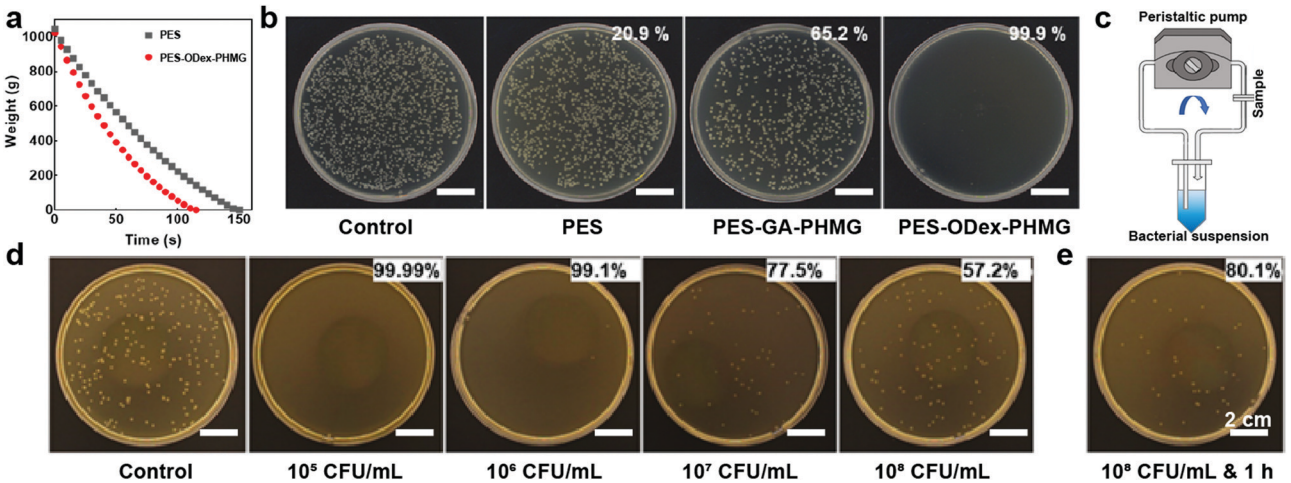

Fig. 3 (a) Water fluxes of PES and PES–ODex–PHMG; (b) filtration efficiencies of PES, PES–GA–PHMG and PES–ODex–PHMG against *E. coli* driven by gravity; (c) illustration of the circular filtration device; (d) 6 min-cyclic filtrations against *E. coli* suspension with different bacterial densities by PES–ODex–PHMG; (e) 1 h-cyclic filtration against *E. coli* suspension at the bacterial density of 10^8 CFU mL^{-1} by PES–ODex–PHMG.

bacteria passed through the MF membrane, it exceeded the instantaneous capture capability of the MF membrane. In order to verify this conjecture, the cycle filtration time of PES–ODex–PHMG was extended to 1 h. As shown in Fig. 3e, the filtration efficiency was increased to 80.1%. This result showed that the filtration efficiency of PES–ODex–PHMG was still increasing as the filtration time increased, even being challenged by high-density bacteria.

The abovementioned results had verified that the PES–ODex–PHMG membranes had good adsorption and interception effects on bacteria. Nevertheless, the intercepted bacteria might induce secondary contamination if they were not inactivated.[38] Therefore, the bacteria on the surface of MF membranes were observed by live/dead staining. After circulating and filtering the *E. coli* suspension at the density of 10^6 CFU mL^{-1} with the MF membrane for 1 hour, the MF membranes were stained with the PI/SYTO 9 staining agent (Fig. 4a). There were almost no bacteria on the PES surface because PES has no adsorption and interception effects on bacteria. On the contrary, more bacteria were observed on the surface of PES–ODex–PHMG. Statistical analysis shows that the proportion of dead bacteria on the surface of PES–ODex–PHMG was 47%, which indicated that PES–ODex–PHMG could inactivate the intercepted bacteria (Fig. 4b). This result indicated that PES–ODex–PHMG could inhibit the growth of bacteria during the serving process, which could alleviate microbial contamination.

In the field of medical and healthcare, since the materials will directly or indirectly contact with the human body, the antimicrobial agents should not be released from the matrix. Therefore, the stability of PES–ODex–PHMG was verified through the inhibition zone test. On the solid culture media of *E. coli* and *S. aureus*, PES–ODex–PHMG had no inhibition zone (Fig. 5a), indicating that the antibacterial mechanism of PES–ODex–PHMG was a non-leaching property, suggesting that PHMG would not be released from the surface. To test the long-term stability, PES–ODex–PHMG was soaked in water for 60 d and used in a filtration experiment against *E. coli* under gravity. The result showed that soaking in deionized water for two months did not affect the filtration efficiency of PES–ODex–PHMG, which demonstrated that PHMG was firmly grafted on the surface (Fig. 5b). Furthermore, the stability of PES–ODex–PHMG was also determined by ultrasonic washing (Fig. 5c). The result indicated that PES–ODex–PHMG had a very high filtration efficiency (99.8%) against bacteria under a high bacterial density of 10^8 CFU mL^{-1} after ultrasonic washing. These results demonstrated the high stability and durability of PES–ODex–PHMG.

In addition, water may be contaminated by other microorganisms, such as algae.[39] In order to verify the effect of PES–ODex–PHMG on the removal of algae, alga filtration experiments were performed. In this experiment, PES–ODex–PHMG was constructed on the PES filtration membrane with the pore size of 10 μm. The photos of filtered algal suspensions showed that the water was clear after filtration by PES–ODex–PHMG, while the suspension filtered by PES still remained green (Fig. 6a). A large amount of chlorella (FACHB-8) was observed on the surface of PES–ODex–PHMG (Fig. 6b). Compared with PES, the OD 450 of the filtrate in the PES–ODex–PHMG group was reduced from 0.6 to 0.02, indicating that PES–ODex–PHMG had excellent filtration ability against chlorella (Fig. 6c). This result proved that PES–ODex–PHMG could efficiently remove other microbes beside bacteria, such as algae.

Moreover, the endotoxin produced by bacterial metabolism is an important pollutant to water.[40] Therefore, it is significant to remove endotoxin from the water. For this purpose, the endotoxin absorption test was performed (Fig. 7a), taking lipopolysaccharide (LPS) as a representative endotoxin. The LPS absorption efficiency of PES–ODex–PHMG reached 59.5% (Fig. 7b). Compared with PES, PES–ODex–PHMG could significantly improve the absorption efficiency of LPS. The improvement of the endotoxin adsorption efficiency of PES–ODex–PHMG was mainly because the positively charged surface could adsorb negatively charged endotoxin through electrostatic interaction.

2.3 Filtration and antimicrobial properties of functionalized PP melt-blown fabrics

PP melt-blown fabrics are widely used for manufacturing PPEs, such as masks. Therefore, it is necessary to determine the filtration efficiency against bacterial aerogel. By counting the bacterial colonies on the sampling plates of the Anderson cascade impactor, the BFE of PP and PP–ODex–PHMG was calculated (Fig. 8a). The BFE of PP–ODex–PHMG against

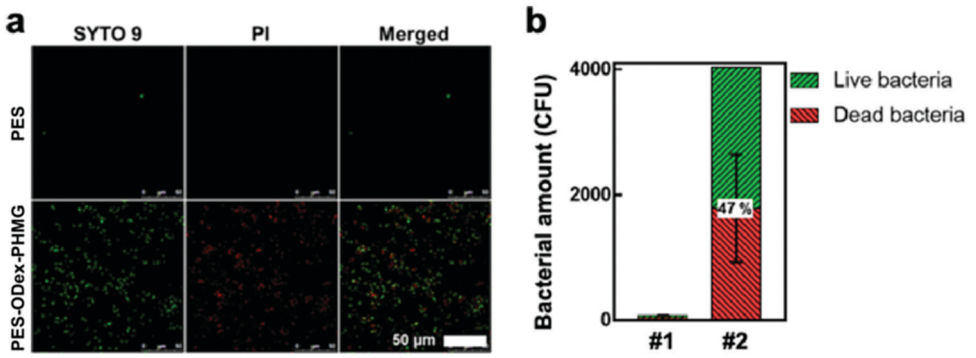

Fig. 4 (a) CLSM images of the bacteria on the surfaces of PES and PES–ODex–PHMG; (b) quantitative statistical data of the bacteria (#1 = PES, #2 = PES–ODex–PHMG).

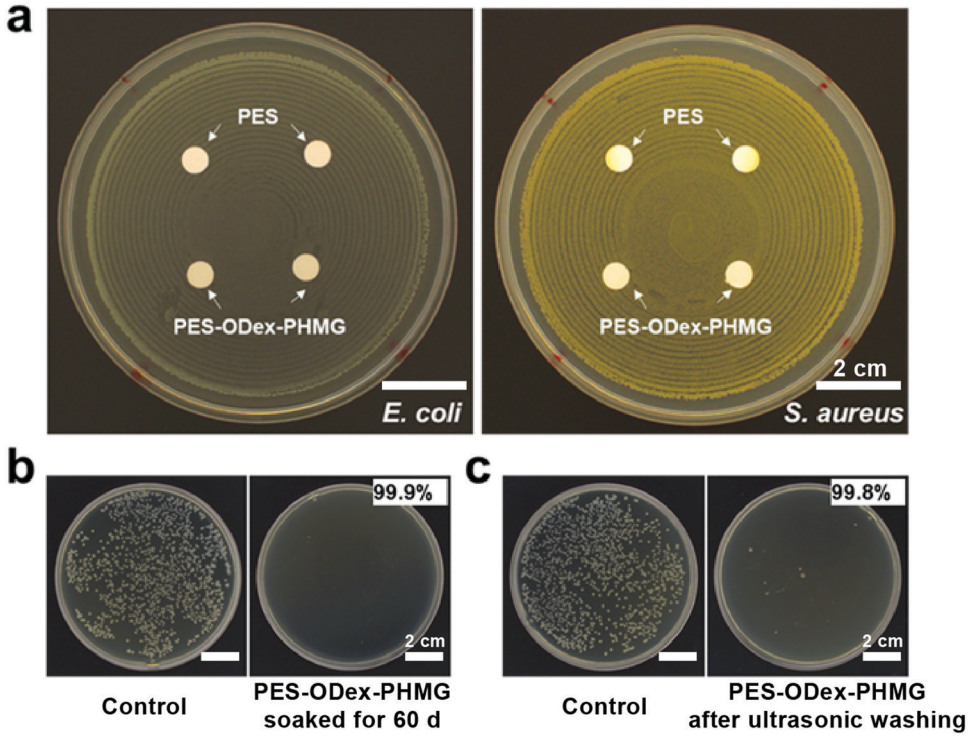

Fig. 5 (a) The inhibition zones of PES and PES–ODex–PHMG; (b) filtration efficiency of PES–ODex–PHMG driven by gravity after being soaked in water for 60 days; (c) filtration efficiency of PES–ODex–PHMG driven by gravity after being washed by ultrasonication.

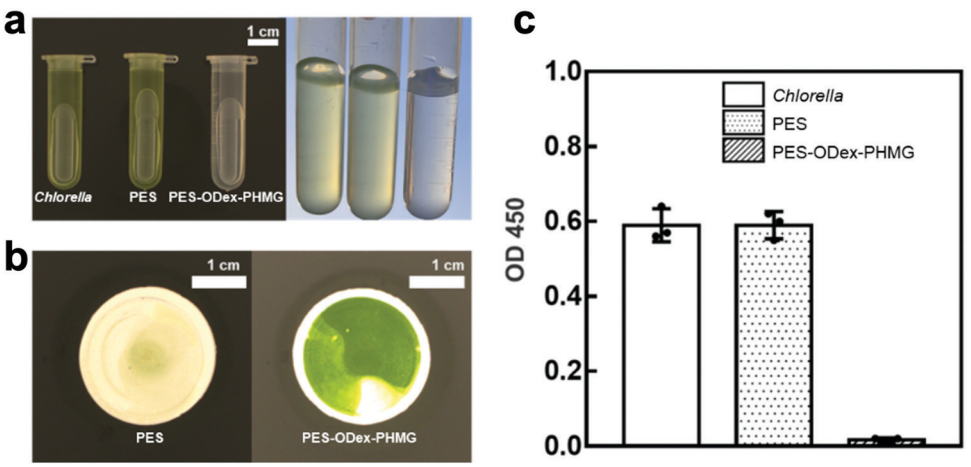

Fig. 6 Filtration experiments for chlorella: (a,b) the status of the pristine and modified MF membranes after filtration; (c) OD 450 of the filtrate.

bacterial aerosols increased from 74.6% to 81.0% (Fig. 8b). This was due to the positive charge of the surface of PP–ODex–PHMG. The purpose of the surface functionalization on the melt-blown fabrics is to impart a higher positive potential on the surface. Therefore, the aerosol particles containing bacteria could be adsorbed and intercepted by electrostatic interaction, which could alleviate the microbial contamination in air and protect the respiratory safety of users.[41]

More importantly, the microbes on the PP melt-blown fabrics would threaten the health of users.[42] Thus, the bactericidal property is essential for the air filtration membranes. The CLSM images of the bacteria on the surface of the melt-blown fabrics were analyzed. After staining with PI/SYTO 9 staining agent, the dead and alive bacteria were observed by red and green fluorescence, respectively (Fig. 9a). Most of the bacteria on the PP surface were live, which indicated that the pristine PP did not have any microbicidal property. After surface functionalization, the ratio of the dead bacteria on PP–ODex–PHMG increased from 17.8% to 92.0% (Fig. 9b), which showed that bacteria on the surface of PP–ODex–PHMG were significantly inactivated. These

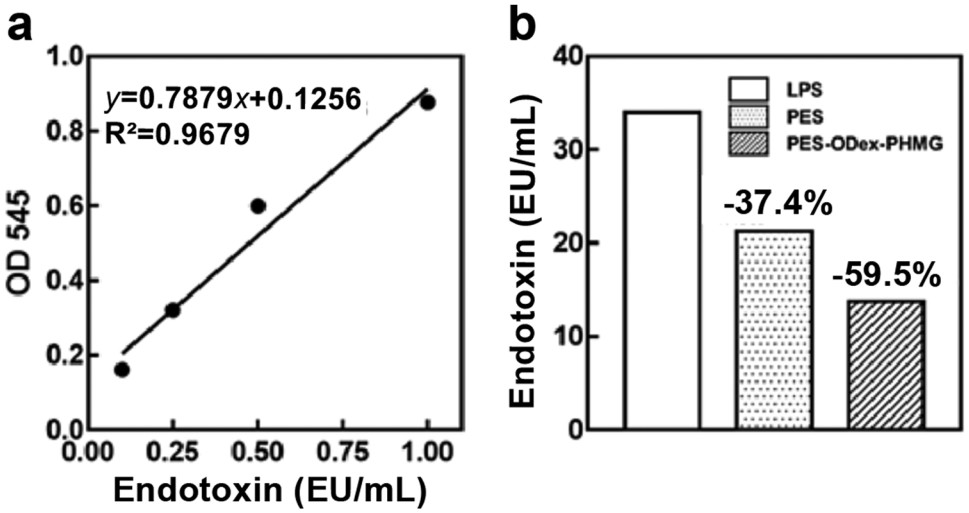

Fig. 7 (a) Standard curve of endotoxin; (b) adsorption capacity for LPS of PES and PES–ODex–PHMG.

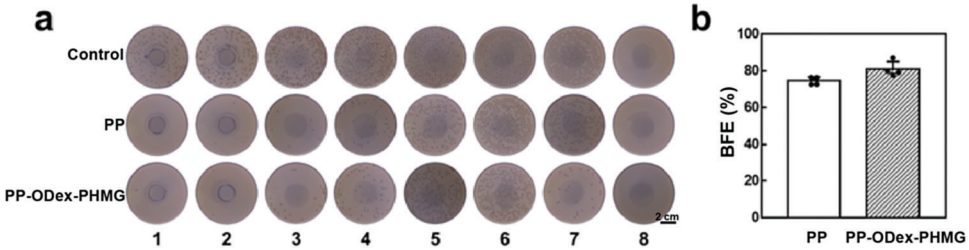

Fig. 8 (a) Colonies on each level of the Anderson cascade impactor; (b) BFE of PP and PP–ODex–PHMG.

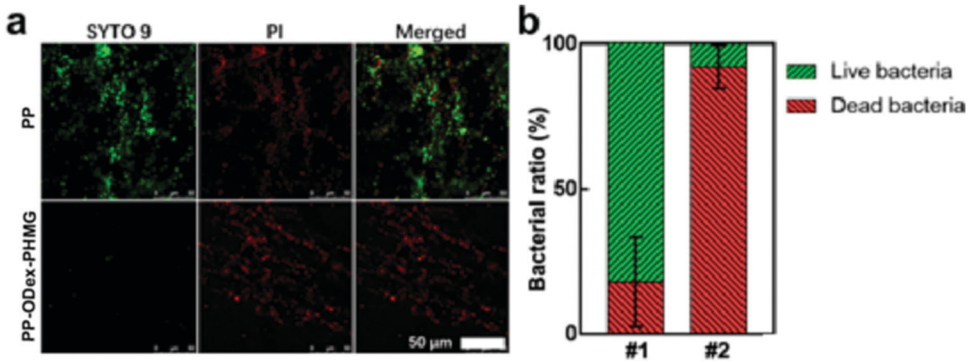

Fig. 9 (a) CLSM images of the bacteria on the surfaces of PP and PP–ODex–PHMG; (b) ratio of dead/live bacteria (#1 = PP, #2 = PP–ODex–PHMG).

results demonstrated the enhanced filtration and microbicidal properties of PP–ODex–PHMG, which was beneficial for air filtration under the condition of the microbial aerogel.

3. Conclusion

In this work, we developed a facile and universal strategy of surface antimicrobial functionalization of two typical filter materials in the medical and healthcare fields. Based on natural polysaccharides, the ODex macromolecular skeleton was constructed on the surface of the filter materials, and an effective antimicrobial agent, PHMG, was covalently grafted on the surface at a high density through Schiff base bonds. By this strategy, stable antibacterial filter materials with high filtration efficiency were fabricated. PES–ODex–PHMG could intercept bacteria and algae in the liquid media, inactivate absorbed microbes, and reduce the amount of endotoxin. PP–ODex–PHMG increased the protection performance against bacterial aerogels, and showed good bactericidal property. The present

work is based on the research of bioinspired surfaces engineering, and obtained water filtration and air filtration materials with good filtration effect and antibacterial efficiency, which provides a new strategy for fighting with antimicrobial contamination in the medical and health field.

4. Experimental Section

The detailed experimental methods are described in the Supporting Information.

Conflicts of interest

There are no conflicts to declare.

Acknowledgements

This work was supported by the National Natural Science Foundation of China (Grant No. 52073024 and 51873012), and Beijing Outstanding Young Scientist Program (Grant No. BJJWZYJH01201910010024).

References

1 C. Buckee, A. Noor and L. Sattenspiel, *Nature*, 2021, **595**, 205–213.
2 S. B. Grant, J. D. Saphores, D. L. Feldman, A. J. Hamilton, T. D. Fletcher, P. L. M. Cook, M. Stewardson, B. F. Sanders, L. A. Levin, R. F. Ambrose, A. Deletic, R. Brown, S. C. Jiang, D. Rosso, W. J. Cooper and I. Marusic, *Science*, 2012, **337**, 681–686.
3 X. L. Zhang, Z. Ji, Y. Yue, H. Liu and J. Wang, *Environ. Sci. Technol.*, 2021, **55**, 4123–4133.
4 G. W. Peterson, D. T. Lee, H. F. Barton, T. H. Epps and G. N. Parsons, *Nat. Rev. Mater.*, 2021, **6**, 605–621.
5 M. A. Schumm, J. E. Hadaya, N. Mody, B. A. Myers and M. Maggard-Gibbons, *JAMA*, 2021, **325**, 1296–1317.
6 Y. I. Kim, M. W. Kim, S. An, A. L. Yarin and S. S. Yoon, *ACS Appl. Mater. Interfaces*, 2021, **13**, 857–867.
7 M. A. Sadique, S. Yadav, P. Ranjan, S. Verma, S. T. Salammal, M. A. Khan, A. Kaushik and R. Khan, *J. Mater. Chem. B*, 2021, **9**, 4620–4642.
8 H. Y. Yang, Z. S. Yan, X. Du, L. M. Bai, H. R. Yu, A. Ding, G. B. Li, H. Liang and T. M. Aminabhavi, *Chem. Eng. J.*, 2020, **382**, 123033.
9 S. F. Anis, B. S. Lalia, M. Khair, R. Hashaikeh and N. Hilal, *Chem. Eng. J.*, 2022, **428**, 131184.
10 B. Rader, L. F. White, M. R. Burns, J. Chen, J. Brilliant, J. Cohen, J. Shaman, L. Brilliant, M. U. G. Kraemer, J. B. Hawkins, S. V. Scarpino, C. M. Astley and J. S. Brownstein, *Lancet Digit. Health*, 2021, **3**, E148–E157.
11 J. C. Wang, S. S. Gao, X. Kang, J. Y. Tian, F. Y. Cui and W. X. Shi, *Mater. Lett.*, 2020, **261**, 127007.
12 D. J. Miller, D. R. Dreyer, C. W. Bielawski, D. R. Paul and B. D. Freeman, *Angew. Chem., Int. Ed.*, 2017, **56**, 4662–4711.
13 X. J. Chen, G. D. Huang, Y. P. Li, C. J. An, R. F. Feng, Y. H. Wu and J. Shen, *Water Res.*, 2020, **181**, 115952.
14 S. Benkhaya, H. Lgaz, S. Chraibi, A. A. Alrashdi, M. Rafik, H. S. Lee and A. El Harfi, *Colloids Surf., A*, 2021, **625**, 126941.
15 R. R. Choudhury, J. M. Gohil, S. Mohanty and S. K. Nayak, *J. Mater. Chem. A*, 2018, **6**, 313–333.
16 H. Shi, E. V. Pasco and V. V. Tarabara, *Environ. Sci.: Water Res. Technol.*, 2017, **3**, 778–792.
17 A. M. C. Maan, A. H. Hofman, W. M. de Vos and M. Kamperman, *Adv. Funct. Mater.*, 2020, **30**, 2000936.
18 X. D. He, G. Sathishkumar, K. Gopinath, K. Zhang, Z. S. Lu, C. M. Li, E. T. Kang and L. Q. Xu, *Chem. Eng. J.*, 2021, **421**, 130005.
19 X. D. He, K. Gopinath, G. Sathishkumar, L. L. Guo, K. Zhang, Z. S. Lu, C. M. Li, E. T. Kang and L. Q. Xu, *ACS Appl. Mater. Interfaces*, 2021, **13**, 20708–20717.
20 S. Y. Wu, J. M. Xu, L. Y. Zou, S. L. Luo, R. Yao, B. N. Zheng, G. B. Liang, D. C. Wu and Y. Li, *Nat. Commun.*, 2021, **12**, 3303.
21 Q. Song, R. X. Zhao, T. Liu, L. L. Gao, C. C. Su, Y. M. Ye, S. Y. Chan, X. Y. Liu, K. Wang, P. Li and W. Huang, *Chem. Eng. J.*, 2021, **418**, 129368.
22 T. R. Sinclair, D. Robles, B. Raza, S. van den Hengel, S. A. Rutjes, A. M. de Roda Husman, J. de Grooth, W. M. de Vos and H. D. W. Roesink, *Colloids Surf., A*, 2018, **551**, 33–41.
23 B. Demir, I. Cerkez, S. D. Worley, R. M. Broughton and T. S. Huang, *ACS Appl. Mater. Interfaces*, 2015, **7**, 1752–1757.
24 X. Ding, S. Duan, X. Ding, R. Liu and F.-J. Xu, *Adv. Funct. Mater.*, 2018, **28**, 1802140.
25 Z. S. Li, S. H. Wang, X. X. Yang, H. Liu, Y. Shan, X. Xu, S. B. Shang and Z. Q. Song, *Appl. Surf. Sci.*, 2020, **530**, 147193.
26 Q. Y. Gu and Z. Q. Jia, *React. Funct. Polym.*, 2013, **73**, 1114–1121.
27 S. Afkham, A. Aroujalian and A. Raisi, *RSC Adv.*, 2016, **6**, 108113–108124.
28 M. He, Q. Wang, W. Zhao and C. Zhao, *J. Mater. Chem. B*, 2018, **6**, 3904–3913.
29 Y. Hu, Y. Li and F. J. Xu, *Acc. Chem. Res.*, 2017, **50**, 281–292.
30 W. Zhao, X. Zhang, R. Zhang, K. Zhang, Y. Li and F. J. Xu, *ACS Appl. Mater. Interfaces*, 2020, **12**, 56898–56907.
31 B. Qiao, J. J. Nie, Y. Shao, Y. Li, C. Zhang, W. Hao, S. Li, D. Chen, B. Yu, H. H. Li, F. J. Xu and J. Du, *Small*, 2020, **16**, e1905925.
32 Y. Liu, N. Zhao and F. J. Xu, *ACS Appl. Mater. Interfaces*, 2019, **11**, 34707–34716.
33 J. J. Nie, B. Qiao, S. Duan, C. Xu, B. Chen, W. Hao, B. Yu, Y. Li, J. Du and F. J. Xu, *Adv. Mater.*, 2018, **30**, e1801570.
34 Z. X. Zhou, D. F. Wei, Y. Guan, A. N. Zheng and J. J. Zhong, *J. Appl. Microbiol.*, 2010, **108**, 898–907.
35 M. S. Brzezinska, M. Walczak, U. Jankiewicz and M. Pejchalova, *J. Polym. Environ.*, 2018, **26**, 589–595.
36 W. Ding, J. Zhou, Y. Zeng, Y. N. Wang and B. Shi, *Carbohydr. Polym.*, 2017, **157**, 1650–1656.
37 Q. Li, Y. C. Yin, D. X. Cao, Y. Wang, P. C. Luan, X. Sun, W. T. Liang and H. L. Zhu, *ACS Nano*, 2021, **15**, 11992–12005.
38 Z. Zhu, Y. Zhang, L. Bao, J. Chen, S. Duan, S. C. Chen, P. Xu and W. N. Wang, *Environ. Sci.: Nano*, 2021, **8**, 1081–1095.

39 H. Wang, G. Z. Qu, Y. S. Gan, Z. Q. Zhang, R. H. Li and T. C. Wang, *J. Hazard. Mater.*, 2022, **422**, 126956.
40 C. Zhang, F. Tian, M. L. Zhang, Z. Q. Zhang, M. Bai, G. Guo, W. J. Zheng, Q. Wang, Y. Shi and L. L. Wang, *Sci. Total Environ.*, 2019, **681**, 365–378.
41 K. Sugihara, *Soft Matter*, 2021, **17**, 10–15.
42 L. Delanghe, E. Cauwenberghs, I. Spacova, I. De Boeck, W. Van Beeck, K. Pepermans, I. Claes, D. Vandenheuvel, V. Verhoeven and S. Lebeer, *Front. Med.*, 2021, **8** 732047.